



## Research Article

# cDC2 and plasmacytoid dendritic cells diminish from tissues of patients with non-Hodgkin orbital lymphoma and idiopathic orbital inflammation

Kamil G. Laban<sup>1,2,3</sup> , Rianne Rijken<sup>3,4</sup>, Sanne Hiddingh<sup>1,2,3</sup>, Jorre S. Mertens<sup>3,4,5</sup>, Rob L. P. van der Veen<sup>2</sup>, Christine A.E. Eenhorst<sup>2</sup>, Aridaman Pandit<sup>3,4</sup> , Timothy R.D.J. Radstake<sup>1,3,4</sup>, Joke H. de Boer<sup>1,2</sup>, Rachel Kalmann<sup>1,2</sup> and Jonas J. W. Kuiper<sup>1,2,3</sup>

<sup>1</sup> Ophthalmology-Immunology Unit, University Medical Center Utrecht, Utrecht University, Utrecht, The Netherlands

<sup>2</sup> Department of Ophthalmology, University Medical Center Utrecht, Utrecht University, Utrecht, The Netherlands

<sup>3</sup> Laboratory of Translational Immunology, University Medical Center Utrecht, Utrecht University, Utrecht, The Netherlands

<sup>4</sup> Department of Rheumatology & Clinical Immunology, University Medical Center Utrecht, Utrecht University, Utrecht, The Netherlands

<sup>5</sup> Department of Dermatology, Radboud University Medical Centre, Radboud University, Nijmegen, The Netherlands

Non-Hodgkin orbital lymphoma (NHOL) and idiopathic orbital inflammation (IOI) are common orbital conditions with largely unknown pathophysiology. To investigate the immune cell composition of these diseases, we performed standardized 29 parameter flow cytometry phenotyping in peripheral blood mononuclear cells of 18 NHOL patients, 21 IOI patients, and 41 unaffected controls. Automatic gating by FlowSOM revealed decreased abundance of meta-clusters containing dendritic cells in patients, which we confirmed by manual gating. A decreased percentage of (HLA-DR<sup>+</sup>CD303<sup>+</sup>CD123<sup>+</sup>) plasmacytoid dendritic cells (pDC) in the circulation of IOI patients and decreased (HLA-DR<sup>+</sup>CD11c<sup>+</sup>CD1c<sup>+</sup>) conventional dendritic cells (cDC) type-2 for IOI patients were replicated in an independent cohort of patients and controls. Meta-analysis of both cohorts demonstrated that pDCs are also decreased in blood of NHOL patients and highlighted that the decrease in blood cDC type-2 was specific for IOI patients compared to NHOL or controls. Deconvolution-based estimation of immune cells in transcriptomic data of 48 orbital biopsies revealed a decrease in the abundance of pDC and cDC populations within the orbital microenvironment of IOI patients. Collectively, these data suggest a previously underappreciated role for dendritic cells in orbital disorders.

**Keywords:** cDC2 · FlowSOM · idiopathic orbital inflammation · non-Hodgkin orbital lymphoma · plasmacytoid dendritic cells



Additional supporting information may be found online in the Supporting Information section at the end of the article.

## Introduction

Non-Hodgkin orbital lymphoma (NHOL), the most common orbital malignancy in adults [1], can be fatal due to metastatic spread. Prompt diagnosis is critical to disease management and prognosis. NHOL can present with similar symptoms as orbital

**Correspondence:** Kamil G. Laban and Jonas J. W. Kuiper  
e-mail: K.G.laban@umcutrecht.nl; J.J.W.Kuiper@umcutrecht.nl

**Table 1.** Demographics of the discovery and replication cohorts

Cohort demographics	Discovery cohort			Validation cohort		
	IOI (n = 13)	NHOL (n = 10)	HC (n = 25)	IOI (n = 8)	NHOL (n = 8)	HC (n = 16)
Discovery cohort						
Female (%)	11 (85%)	5 (50%)	18 (72%)	6 (75%)	5 (63%)	10 (63%)
Age (years); mean ±SD	45.9 ± 14.8	60.6 ± 9.7	43.6 ± 14.1	48.5 ± 17.2	64.9 ± 17.3	47.9 ± 10.7
NHOL subtype, n (%)						
EMZL	–	7 (70%)	–	–	4 (50%)	–
DLBCL	–	1 (10%)	–	–	1 (13%)	–
Follicular	–	1 (10%)	–	–	2 (25%)	–
Other	–	1 (10%)	–	–	1 (13%)	–
Location						
Lacrimal Gland	10 (77%)	3 (30%)	–	3 (38%)	–	–
Orbit	3 (23%)	5 (50%)	–	5 (63%)	7 (88%)	–
Conjunctiva	–	2 (20%)	–	–	1 (13%)	–

Abbreviations: IOI, idiopathic orbital inflammation; NHOL, non-Hodgkin orbital lymphoma; HC, healthy control; EMZL, extranodal marginal zone lymphoma; DLBCL, diffuse large B-cell lymphoma. Other NHOL types: discovery cohort, small lymphocytic lymphoma; replication cohort, mantle-cell lymphoma.

inflammatory disease, such as idiopathic orbital inflammation (IOI), the most common non-thyroid associated orbital inflammatory disorder [2–7]. Differentiating between the two can be difficult, particularly when histopathology is inconclusive or when an incisional biopsy is difficult to obtain due to deep orbital localization [8].

Although little is known about the pathophysiology of IOI, infiltration of B- and T-cells is considered a hallmark for this condition [9]. In contrast, NHOL is in almost all cases a B-cell malignancy caused by genetic translocations that affect the *NFKB1*, *BCL2*, *BCL6*, *MYC*, *EZH2*, or *MEF2B* genes, which result in B-cell hyper-proliferation [1]. Curiously, lymphoma occurs more frequently among patients with immune disorders characterized by B-cell hyperactivity, such as primary Sjögren's syndrome, a condition that may also affect the orbital cavity [1]. B cells repeatedly rearrange their genome by the variable (V), diversity (D), and joining (J) gene recombination, somatic hypermutation, and class switch recombination to be able to generate unique antigen receptors. However, these unique properties are not completely error-free and make B-cells vulnerable to transformation. The current view is that inflammatory conditions promote B-cell receptor activation and complex cellular signaling, which enhances the survival of potential malignant B cell clones and the development of lymphoma [1, 10–12]. This suggests that IOI and NHOL may have overlapping molecular mechanisms. Interestingly, marginal zone lymphomas such as primary cutaneous marginal zone lymphoma, have, in addition to the B-cell proliferation, an increase in plasmacytoid DCs (pDCs) arranged in larger clusters with unknown function [13]. As the extranodal marginal zone lymphoma (EMZL) is the most common NHOL subtype [14], pDCs could therefore also be involved in NHOL.

A recent study investigating flow cytometry of orbital biopsies demonstrate that the composition of B- and T-cells in orbital tissue is changed in NHOL and IOI patients [15]. However, it remains to be determined if PBMCs are also affected in these orbital conditions. Changes in immune cells as determined by flow cytometry

of PBMCs may reveal new insights in the complex pathophysiology underlying orbital diseases that are currently largely unknown. To this end, we used flow cytometry to phenotype common and rare myeloid and lymphocyte populations in blood of two cohorts of NHOL and IOI patients and unaffected controls. Additionally, in an attempt to explain circulatory differences, we investigated local cellular composition by deconvoluting orbital transcriptomic data.

## Results

### Quality control

Detailed demographic information for the NHOL and IOI groups are presented in Table 1. In the discovery cohort, we performed standardized flow cytometry analysis of PBMCs in eight independent batches (Fig. 1A). We assessed the data consistency within the batches by calibration beads and principle component analysis of manually gated data with internal control samples. Tracking by calibration beads revealed a stable performance in all channels across the batches (Fig. 1B). Principal component analysis revealed clustering of the internal control samples, which suggests stable variance across all experiments (Fig. 1C). Therefore, we removed the internal control samples and combined the eight batches for self-organizing-map-based gating by FlowSOM for comprehensive and unbiased mapping of all leukocyte populations.

### NHOL and IOI are characterized by decreased circulating DC populations

FlowSOM considers all surface markers (in a cytometry panel) across all cells simultaneously, and uses unsupervised learning based on self-organizing maps (SOM) and hierarchical consensus

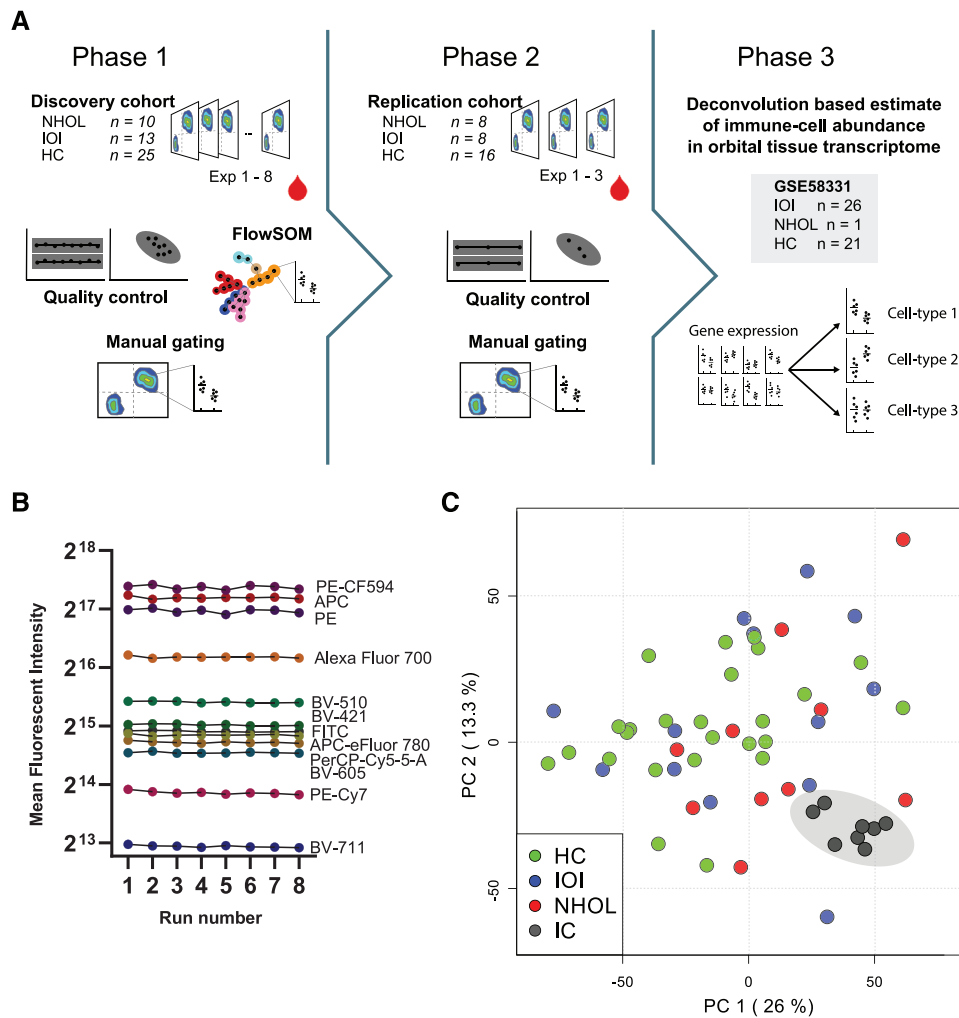


**Figure 1.** Study design and quality control. (A) Study design. High-dimensional immune profiling was performed in frozen PBMCs of patients with NHOL, IOI, and controls in two independent cohorts. Data from eight flow cytometry experiments (discovery cohort) were combined for automatic gating by FlowSOM. The populations identified by FlowSOM were confirmed by manual gating (Phase 1,  $n = 48$ ). An independent cohort (Phase 2,  $n = 32$ ) was used to replicate the observations from Phase 1. In Phase 3, we analyzed orbital biopsies transcriptomic data for immune cell genes and used deconvolution algorithms to assess the relative immune cell abundance in the orbital microenvironment. (B) Mean fluorescent intensities for (rainbow) calibration beads across the eight experiment of Phase 1. (C) The first two principal components of the manually gated data of the discovery cohort ( $n = 48$ ) and internal controls ( $n = 8$ ). The gray ellipse highlights the cluster of the internal control samples. Abbreviations: Exp, experiment; HC, healthy control; IOI, idiopathic orbital inflammation; NHOL, non-Hodgkin orbital lymphoma; IC, internal control; PC, principle component.

meta-clustering to map all phenotypically similar cell clusters in a 2D spanning tree. Group differences and head-to-head comparisons for all meta-clusters are shown in Supporting Information Table S1.

For the mononuclear myeloid and dendritic cell panel, FlowSOM distinguished 17 meta-clusters (Fig. 2A) of which four (A1–A3, A5) showed a different abundance between the groups at nominal significance ( $p < 0.05$ ). Meta-clusters A2 ( $CD14^+CD16^+CD11c^+$ ) represented classical monocytes and were increased in the NHOL group compared to the IOI group. Meta-clusters reminiscent of pDCs (A5,  $HLA-DR^+CD303^+CD123^+$ ), were less abundant in IOI and NHOL compared to controls, while meta-clusters for conventional dendritic cells (cDC) type-2 (A3,  $HLA-DR^+CD11c^+CD1c^+$ ) were specifically decreased in the IOI

group, also compared to NHOL cases (Supporting Information Table S1).

FlowSOM analysis of the T-cell panel (Fig. 2B) revealed a different abundance for three of 16 meta-clusters. This was the result of a decrease in the abundance of  $CD8^+CD27^+$  T-cells in patients (meta-cluster B1, which also contained populations with moderate CXCR3 expression), a decrease in a meta-cluster driven by  $CD8^+CD45RO^+CD27^+CD161^+CCR6^+$  T-cells (B2), and lower abundance for a meta-cluster defined by a decrease in double negative ( $CD4^-CD8^-$ ) T cells (B3) in NHOL patients.

In the B-cell panel (Fig. 2C), we observed changes in four of 18 meta-clusters (C1–C4), of which two meta-clusters of B cells that express CD27 and CD38 (C3 and C4). Note that the increase in abundance of meta-clusters C1 and C2 most likely represents an

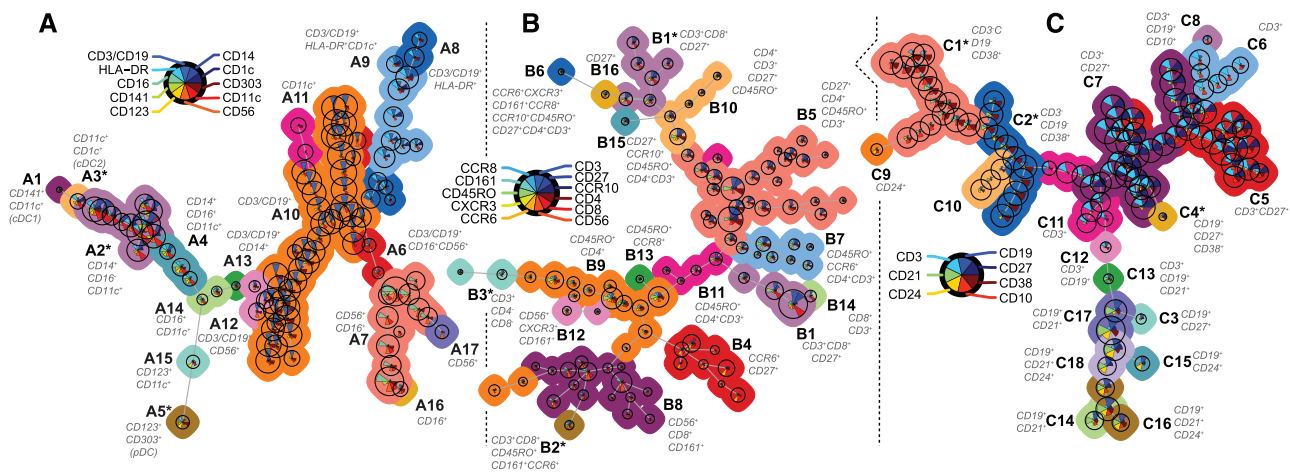


**Figure 2.** Automatic gating by FlowSOM for unbiased leukocyte composition mapping in orbital disease. FlowSOM tree for mononuclear myeloid and DC panel (A), the T-cell panel (B), and the B-cell panel (C) in 48 PBMC samples for the discovery cohort. Unsupervised clustering was used to identify meta-clusters (displayed by a unique color) that represent related cell-lineages in the PBMC compartment (A1–C18). The size of the pie-chart is relative to the cluster size (i.e., percentage of the single cell gate). The star charts visualize the relative surface marker expression used to distinguish the clusters. Meta-cluster B3 contains double negative T-cells ( $CD4^-CD8^-$ ) and NKT-cells. Group differences for each meta-cluster are indicated by “\*” and details are shown in Supporting Information Table S1.

increase in monocytes ( $CD3^+CD19^-CD38^+$ ), because these clusters show strong correlation with the monocyte meta-clusters (e.g., meta-cluster A2 versus C2, Spearman’s  $\rho = 0.80$ ,  $p < 0.001$ ).

Next, we were interested to validate these observations using manual gating. Manually gating data confirmed the increase in ( $CD14^+CD16^+CD11c^+$ ) classical monocytes and decrease in  $CD3^+CD8^+CD27^+$  and  $CD3^+CD8^+CD45RO^+CD161^+CCR6^+$  T cells in NHOL patients. We also confirmed the decrease in pDCs in NHOL and IOI patients compared to controls and confirmed the decrease in cDC type-2 in IOI patients (Fig. 3). None of the changes within the B cell population identified by FlowSOM were confirmed by manual gating (Supporting Information Table S2).

### An independent cohort confirms a decrease in DC subsets for patients

Next, we conducted flow cytometry in an independent cohort of 16 patients and 16 controls to replicate the findings of the first cohort (Table 1). We replicated the decrease in pDCs in IOI compared to controls (Supporting Information Table S2; Fig. 3), and the decrease in cDC type-2 in IOI patients with consistent direction of effect in the second cohort. In contrast to the other leukocyte populations investigated, DCs are rare within the single cell gate. Since this might affect power to detect group differences, we also evaluated the percentage of pDCs and cDC type-2 cells in the conventional lineage-negative ( $CD3^-/CD19^-/CD56^-/CD14^-$ ) HLA-DR-positive gate of the combined cohorts (Supporting Information Fig. S1). This analysis confirmed the decreased expression of these DC populations in IOI (adjusted  $p = 1.78 \times 10^{-3}$ ), and ascertains also the decrease in pDCs in NHOL compared to controls (adjusted  $p = 1.48 \times 10^{-4}$ ). Analysis of the combined manual gated data of both cohorts also supports a specific decreased of cDC type-

2 cells in IOI compared to NHOL (adjusted  $p = 2.77 \times 10^{-2}$ ), which is in line with the initial observations by FlowSOM. Although age and sex differences are intrinsic to the diseases studied (Table 1), the effect of age or sex on the difference in abundance of dendritic cells in blood was negligible (Supporting Information Table S3). In summary, we demonstrated a consistent decrease in circulating DCs, especially pDCs, in NHOL and IOI.

### DC alterations in biopsy material

Next, we were interested to explore the potential role of dendritic cells in the microenvironment of IOI. To this end, we investigated the transcriptome of orbital biopsies of 26 IOI patients and 21 controls. Available data from one NHOL patient was used for visualization only. Gene expression profiles revealed that various signature genes for cDCs (e.g., *CSF1R*, *NDRG2*) and pDCs (e.g., *NRP1*, *PTGDS*) are well expressed in biopsy tissues of patients and controls (Fig. 4A). Differential expression analysis revealed that the expression of several of these DC signature genes (e.g., *NRP1*, *CSF1R*, *PTGDS*) are also changed in patients with IOI compared to controls (Fig. 4B). Deconvolution approaches can be applied to bulk gene expression data to infer cellular composition of complex tissue mixtures [16]. We estimated the cellular fraction of cDCs and pDC from the gene expression data from IOI cases and controls using deconvolution-based estimation with CIBERSORT [17], and estimated the fraction of B-cells as an internal control. B cells are well known to be increased in biopsies of IOI patients [1, 8]. Because the leukocyte signature matrix often used for CIBERSORT (called LM22) does not contain reference data for pDC or cDCs, we used a signature data from a recently developed deconvolution algorithm “Absolute Immune Signal” (ABIS) trained on pDC and cDC data. As expected, the relative fraction of B cells in biopsy

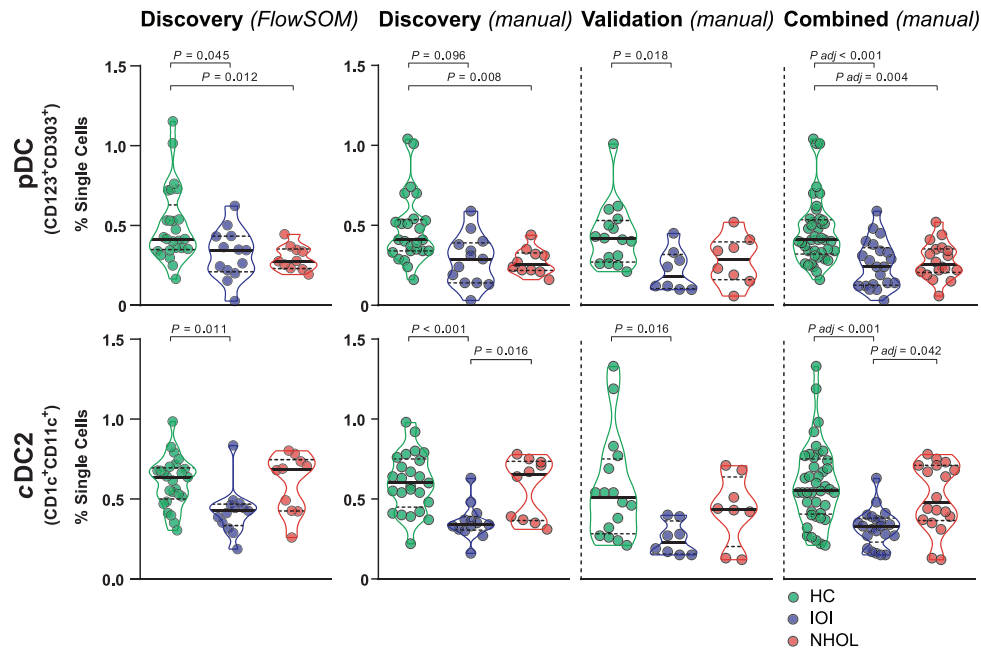


**Figure 3.** pDC and cDC2 populations in patients and controls. The percentage of pDC and cDC2 in the single cell gate for automatic gating with FlowSOM, and manual gating. Data for the discovery, validation, and combined cohorts are indicated. The Kruskal–Wallis tests with Dunn’s post hoc test were used to assess differences between groups. The adjusted *P*-values are corrected using the Benjamini–Hochberg method. The median with interquartile ranges are indicated by black lines and dotted lines, respectively. Abbreviations: HC, healthy control; IOI, idiopathic orbital inflammation; NHOL, non-Hodgkin orbital lymphoma; pDC, plasmacytoid DCs; cDC2, conventional DCs type-2; *p*, nominal *p*-value; *p* adj, adjusted *p*-value.

material of IOI patients was increased ( $p = 0.002$ ), because no B cells were estimated to be present in the control biopsies. Also, the relative proportion between cases and controls was very similarly estimated by CIBERSORT using either LM22 or ABIS signature sets (Fig. 4C). Finally, the biopsies were estimated to contain heterogeneous fractions of pDCs and cDCs, indicating that DCs constitute the orbital microenvironment. Importantly, we observed a decrease in the estimated fraction of pDCs and cDCs (Fig. 4D) in IOI cases compared to controls. In summary, the results suggest that orbital inflammation of IOI is associated with decreased DC populations in the ocular microenvironment.

## Discussion

In this study, we observed decreased pDCs in peripheral blood of patients with IOI and NHOL, and a specific decrease in cDC type-2 cells in IOI patients, also compared to NHOL. Deconvolution-based estimation suggests that the drop in circulating dendritic cells in IOI patients can be accompanied by a lower abundance of these DC populations in the orbital microenvironment.

The contribution of dendritic cells to NHOL and IOI is currently unknown. Our analysis suggests that the abundance of these cells in blood and their gene expression in orbital tissues is altered, which warrants further functional analysis of these populations to better understand their contribution to orbital pathology. This could reveal new possibilities for future diagnostic and therapeutic strategies for NHOL and IOI management.

DCs are APCs that can initiate and drive immune responses in various human pathologies [18]. Although various subpopulations of DC populations are distinguished, much of their functional specialization during malignancy or inflammatory disease in humans remains to be elucidated.

The classical dogma considers discrete functions for DC subsets with pDC effective in recognizing viral or endogenous nucleotides (e.g., DNA, RNA) upon which large amounts of INF are produced to induce inflammation [18]. The cDCs are considered important for the recognition of intracellular and extracellular pathogens and present exogenous Ags to T-cells [18]. In reality, however, the redundancy in function and magnitude of influence on immune responses is complex and context-dependent. Regardless, the significant role of dendritic cells in human disease has been unequivocally demonstrated; DCs play an important role in antitumor response toward malignant cells and are drivers of various severe inflammatory conditions [19–21].

Similar to our results, a decrease in blood DCs is observed in inflammatory disorders, such as systemic lupus erythematosus [22] and the eye condition uveitis [23]. Also, a reduction in DC numbers in blood has been documented in patients with leukemia [24–27], multiple myeloma [28], classical Hodgkin lymphoma [29], and other types of cancer [30]. This phenomenon could be part of an immunosuppressive state caused by the tumor microenvironment, triggered by metabolic stress, hypoxia, or secretion of cytokines and alarmins that affect DCs [30]. Although in our analysis of the single cell gate did not show a consistent decrease of pDCs in NHOL patients, evaluation of this rare cell population



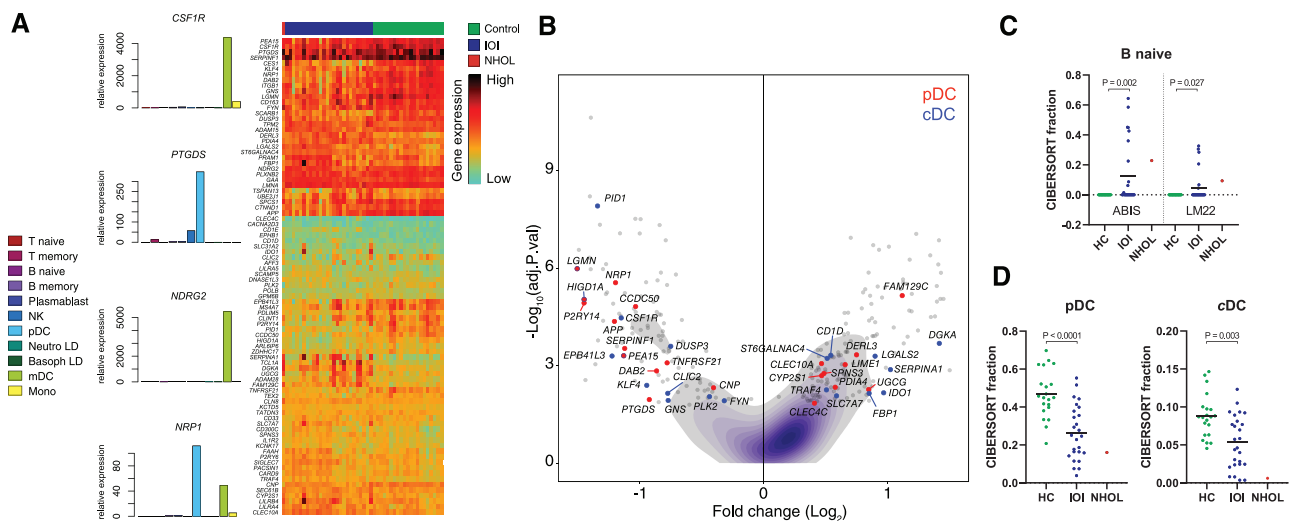


**Figure 4.** Dendritic cell gene signatures are present in orbital biopsies. (A) Gene expression profile of signature genes [16] of pDC and cDC in orbital biopsies of 26 IOI patients and 21 controls (GSE58331). The specificity of several hallmark genes for cDCs and pDCs are indicated by the barplots on the left. A larger version of the heatmap is available in the Supporting Information Fig. S2. (B) A volcano plot of the gene expression changes of 794 genes in orbital biopsies of 26 IOI patients versus 21 controls (data obtained from GSE58331). The density contour indicates the density estimation of the fold change in expression and p-values for the genes. Differentially expressed genes ( $-\log_{10}$  of the FDR adjusted p-values from differential expression analysis in *limma*) are indicated by dots. Differentially expressed signature genes [16] for pDC and cDC subsets are highlighted in red and blue, respectively. Genes linked to both cDC and pDCs are indicated by both red and blue. (C) Deconvolution-based estimation by CIBERSORT of the fraction of naive B cells (using ABIS or LM22 as signature sets to estimate the cell fraction) in biopsies of IOI and controls, and one NHOL sample. (D) Deconvolution-based CIBERSORT estimation of pDC and cDC fractions (ABIS signature set used) for the same samples as in (C). The Mann–Whitney *U* test was used to assess differences between groups. Group means are shown. Abbreviations: HC, healthy control; IOI, idiopathic orbital inflammation; NHOL, non-Hodgkin orbital lymphoma; NK, Natural Killer cells; neutroph LD, low-density neutrophils; basoph LD, low-density basophils; mono, monocytes; pDC, plasmacytoid DC; cDC, conventional DC.

in more conventional gates for manual gating (lineage-negative HLA-DR-positive cell gate) showed a consistent decrease of pDCs in NHOL. The role of pDCs in cancer is supported by the observation of pDC restoration in peripheral blood in patients under anticancer treatment [29]. In contrast to pDC associated conditions such as primary Sjögren's syndrome and systemic sclerosis that show accumulation of pDCs at the side of inflammation [22], we observed a moderate decrease in the estimated pDC numbers in biopsies. Here, it is important to consider that it was previously found that pDCs in mice can be segregated into multiple populations with functional differences. For example, pDCs with tolerogenic functions control T regulatory formation to maintain tolerance in mucosal sites [31]. Interestingly, pDCs are known to regulate B cell differentiation and Ig secretion through CD70 and IL-6 [32]. The lower number of pDCs locally in concurrence with B cell infiltrate in IOI could therefore be driven by a negative feedback loop mediated by self-maintaining B-cell expansion, or pDC differentiation and activation affecting surface marker expression [19]. In blood, however, we observed no correlation between DC subtypes and the B-cell compartment.

In this study, we use a three-phase strategy to determine the changes in immune cells of NHOL and IOI. However, some limitations need to be addressed. Due to the rare and heterogeneous nature of orbital disease, clinical variation exists and may influence our observations. For example, analysis of NHOL subtypes would be highly desirable, but considering the rare occurrence of disease, it is difficult to obtain sufficient number of samples

to pursue such analysis. Three NHOL patients with a history of lymphoma in remission were comparable to other samples in the NHOL group. As with any idiopathic condition, the diagnosis IOI is established after exclusion of any known cause for orbital disease. Although future studies may proof distinct subtypes within the IOI group, there are currently no robust molecular subtypes of IOI that we could take along in our studies [33].

Also, we demonstrated that transcriptomic signatures of orbital tissues show signature genes for DCs. For example, the expression of *NDRG2* and *CSF1R* suggests the presence of cDCs. N-myc downstream-regulated gene 2 (*NDRG2*) is a differentiation-related gene specifically linked to cDCs [34] and *CSF1R* expression is typically associated with cDC differentiation [35]. However, these genes are also implicated in monocyte to DC differentiation and we cannot conclusively state that the expression is limited to cDCs only in tissues. Also, as far as we are aware there is currently no transcriptomic data available that is trained to deconvolute cDC type-1 and cDC type-2 in (orbital) tissues. Future studies using single cell sequencing are warranted to dissect the subtle differences between monocyte derived inflammatory dendritic cells and cDCs in tissues.

Third, although the genes linked to pDCs such as *NRP1* and *PTGDS* are also expressed by non-hematopoietic cells, the changes in their gene expression in orbital tissue and circulating number of pDCs suggest that these observations may be causally linked in the etiology of orbital disease. This is supported by the (multigene signature) deconvolution of the orbital transcriptome,

which demonstrated a decrease in pDCs and cDCs in tissues of IOI patients, similar to the results from flow cytometry in blood. Also, using estimation of cell numbers, we confirm enrichment for B cells in orbital tissues—a phenomenon well documented in IOI and NHOL [1, 8]. However, we emphasize that further research is needed to quantify the DC populations in orbital biopsies. Deconvolution methods based on gene expression profiles assume that the bulk gene expression profile constitutes the weighted sum of the cell type-specific transcriptomes. Although such algorithm-based strategies have revolutionized our understanding of the rich composition of biopsies, some cell types are very poorly deconvoluted in progressively complicated tissues. Also, patient-to-patient variability—as a result of difficulty in taking a representative orbital biopsy—will influence any deconvolution method, in particular for cell subsets that are difficult to distinguish due to data collinearity (i.e., having similar expression profiles). Future work in NHOL and IOI may benefit from benchmarking deconvolution methods by single cell sequencing data from orbital biopsies.

In conclusion, we discovered that DCs are reduced in peripheral blood of patients with NHOL and IOI and altered in the disease microenvironment. These results unveil a potentially novel role of DCs in orbital disease that warrants replication and functional understanding to determine its relevance for future diagnostic and treatment purposes.

## Methods

### Patients

In total, 39 patients and 41 controls (HC) were included in this study. Blood was collected from patients recruited at the University Medical Center Utrecht, Utrecht, The Netherlands between February 2015 and May 2018. Forty-one (self-reported) healthy control samples were obtained from a pool of employees of the University Medical Center Utrecht that provide voluntary unpaid blood donations for research purposes (Approved by the institutional review board). We immunophenotyped a discovery cohort (NHOL:  $n = 10$ , IOI:  $n = 13$ , HC:  $n = 25$ ) and 1 year later an independent validation cohort (NHOL:  $n = 8$ , IOI:  $n = 8$ ; HC:  $n = 16$ ). This study was conducted in accordance with the Declaration of Helsinki and was performed with approval of the Institutional Review Board of the University Medical Centre Utrecht, The Netherlands (protocol #14-065). All patients included in this study gave written informed consent before participation.

All cases of NHOL were diagnosed and classified following WHO criteria with histopathological assessment of incisional biopsies [36] (see Table 1 for details). Histopathologic examination of NHOL included assessment of B cell and T cell specific markers (CD3, CD5, CD20, CD79 $\alpha$ ) and specific B cell subset markers (BCL2, BCL6, CD10, CD23, CD30, Cyclin D-1, MUM-1, and  $\kappa$  and  $\lambda$  light chains) for NHOL subtyping. PCR-based clonality analysis was used and revealed monoclonality for NHOL, except two NHOL patients that showed a monotypic  $\lambda$  light chain expansion

in histopathology. In addition, translocations were assessed by fluorescence in situ hybridization in patients with diffuse large B-cell lymphoma (DLBCL).

IOI, a diagnosis of exclusion, was considered in patients with an orbital mass without evidence of infection, lack of evidence for granulomatosis with polyangiitis, sarcoidosis, primary Sjögren's syndrome, benign lymphoid hyperplasia, IgG4-related pathology, histiocytic disease, or malignancy [8, 37]. Note histopathological confirmation of incisional orbital biopsies was obtained for all patients, except for six patients with idiopathic myositis. In all IOI biopsies, a non-specific polymorphous plasmalymphocytic infiltrate was seen, negative for IgG4, with or without the presence of neutrophils, eosinophils, histiocytes, and macrophages, and varying amounts of fibrosis in the connective tissue. Idiopathic myositis patients were diagnosed based on the presence of pain, diplopia, (paretic) motility reduction and pain with eye-movement, negative laboratory findings (e.g., no autoantibodies and normal serum IgG4 levels), and extra-ocular muscle swelling with contrast-enhancement on magnetic resonance imaging [8, 37].

All patients were diagnosed by an ophthalmologist specialized in orbital diseases. All patients had blood withdrawal at time of diagnosis and had active disease. Treatment was not yet initiated at the time of blood withdrawal. Additionally, none of the patients received systemic corticosteroids 3 months—or immunomodulatory treatment in the past 6 months—prior to blood withdrawal, except for one patient of the validation cohort (low dose of 2.5 mg oral prednisolone daily). Also, patients had not received radiation treatment or chemotherapy in the previous year before sampling.

### Flow cytometry

The study design is depicted in Fig. 1A. PBMCs were isolated by standard ficoll centrifugation of whole blood obtained by lithium heparin vacutainers (#367880, BD Vacutainer, BD Bioscience, USA) and stored overnight at  $-80^{\circ}\text{C}$  using a freezing container (#BCS-405, CoolCell LX, Biocision, USA) and subsequently stored at liquid nitrogen. The two cohorts were measured separately 1 year apart. PBMC samples were measured by flow cytometry in batches of five to 12 samples per run, divided over 8 days for the first cohort and 3 days for the second cohort, 1 year apart. Per batch, 10 million PBMCs per sample were quickly thawed, washed with ice cold PBS and divided for staining with three antibody panels (see Supporting Information Table S4) with a specific amount of cells per panel; a mononuclear myeloid panel (1.9 million cells), a B cell panel (300 000 cells), and a memory T-cell panel (400 000 cells). PBMCs were incubated with 5% heat-inactivated mouse serum at room temperature for 15 min to reduce non-specific antibody binding. Cells were then plated in V-bottomed plates (#651101, Greiner Bio-one, Germany), washed with PBS supplemented with BSA (1%) and incubated for 20 min at  $4^{\circ}\text{C}$  in the dark with Brilliant Stain Buffer (#563794, BD Horizon, BD Bioscience, USA) and the fluorescently-conjugated antibodies. Next, the cells were washed and taken up in PBS supplemented with BSA (1%) and 0.1% sodium azide.

Flow cytometric analyses were performed on the BD LSR Fortessa™ Cell analyzer (BD Bioscience, USA), in adherence to previous reported guidelines [38]. Manual gating of blinded data (i.e., coded samples) was done in FlowJo software (TreeStar Inc., USA). An example of the gating strategy basis is provided under Supporting Information Fig. S3. Flow cytometer calibration was monitored before and after every run using eight peak Sphero™ Rainbow Calibration particles (#RCP-30-5A, Spherotech Inc., USA). The relative SD calculated with the coefficient of variation was <5% for all fluorescently conjugated antibodies across individual runs for the discovery and the validation cohorts, and <10% for both cohorts combined. Interassay variation was determined using aliquots of one control sample in each run in both cohorts. Across all runs the sample revealed relatively low interassay variation, showing a relative SD of <15% within all common leukocyte populations (population size >5% of single cells). Principle component analysis confirmed the high consistency of the individual runs (Fig. 1B). After inspection of the manual gated data, we excluded CCR4 from the T-cell panel, because the overall fluorescent intensity for this chemokine receptor was indistinguishable from the Fluorescence Minus One control experiment. Note that we further expanded the B cell panel with antibodies directed to surface Igs in the second cohort (Supporting Information Table S4).

### FlowSOM and Statistical analyses

Flow cytometry data were visualized with SOM clustering and Minimal Spanning Trees using the *FlowSOM* [39], as described previously [23]. Briefly, single cell data (FSC-A versus FSC-H gates) were transformed using the *logicleTransform* function of the *flowCore* package [40]. The SOM was trained for a grid size of 100 (populations) with 2000 iterations. Consensus hierarchical clustering was used to annotate clusters, based on the *ConsensusClusterPlus* R package [41]. FlowSOM subsequently determined the appropriate number of (maximum 90 color-coded) meta-clusters using the Elbow criterion method. Meta-clusters represent lineages and closely related cell populations. Identified clusters that represented <0.1% of all single cells were ignored to prevent potential overfitting. Head-to-head comparison of the frequency of meta-clusters between the groups was performed using the Kruskal–Wallis test with subsequent Dunn’s Bonferroni-corrected post hoc test in R 3.5 using the *FSA* package and *dunnTest* function. Group differences identified by *FlowSOM* at a nominal  $p < 0.05$  were confirmed by manual gating (populations expressed as % of single cell gate) and considered validated if the group differences replicated at a nominal  $p < 0.05$  and if these observations replicated at a nominal  $p < 0.05$  and showed consistent direction of effect in an independent cohort of patients and controls. We combined manual gated data from cohort 1 and 2 for meta-analysis and corrected the  $p$ -values for multiple comparisons using the Benjamini–Hochberg method. For quality control, we conducted principal component analysis of manual gated data with *MetaboAnalyst v4* [42]. Group data were reported as median with interquartile range. Violin plots

were generated with Graphpad Prism version 8. 0 (GraphPad, La Jolla, CA, USA).

### Orbital tissue transcriptome analysis and deconvolution

Gene expression data (Affymetrix U133Plus2 array) of 48 orbital cavity biopsies from IOI patients ( $n = 26$ ) and a NHOL patient ( $n = 1$ , only used for visualization), and surgically residual orbital material from unaffected orbits ( $n = 21$ ) were obtained from the NCBI Gene Expression Omnibus (accession number GSE58331) [33, 43]. The Affymetrix CEL files were simultaneous preprocessed and a differential expression analysis was conducted on all samples. Data were interrogated by GEO2R [44] from the GEO database, which builds on the *GEOquery* and *limma* R packages (i.e., differential expression analysis). The differential expression by the *limma* package uses a linear model on  $\log_2$  transformed and quantile normalized data using *lmFit* function and adjusts  $p$ -values according to the Benjamini–Hochberg method. For deconvolution of the bulk patient profiles, expression profiles were analyzed by CIBERSORT [17] to estimate the cell fractions for pDC, cDC, and B cells in biopsy material. Because the CIBERSORT standard reference signature expression matrix for leukocytes (LM22) does not contain data for pDC and cDC subsets, we used microarray signature data from ABIS [16]. According to previous suggestion, output was processed by replacing negative numbers by zeros [17]. We used the estimated fraction of pDCs, cDC, and naïve B-cells for comparison between IOI and controls. We extracted the top 50 genes with the highest signal for pDCs and cDCs (87 unique genes) from the signature microarray reference of ABIS from the transcriptomic data to investigate the relative expression of DC genes in orbital biopsies.

**Acknowledgements:** We would like to thank Maarten Mourits and Stijn Genders for their assistance in the recruitment of patients. This study was supported by unrestricted grants from the Dr. F.P Fischerstichting, Stichting Lijf & Leven, Rotterdamse Stichting Blindenbelangen, and Stichting Ankie Hak. The funders had no role in study design, data collection and analysis, decision to publish, or preparation of the manuscript.

**Conflict of interest:** The authors declare no financial or commercial conflict of interest.

### References

- Olsen, T. G. and Heegaard, S., Orbital lymphoma. *Surv. Ophthalmol.* 2019. 64: 45–66.



- 2 Gordon, L. K., Orbital inflammatory disease: a diagnostic and therapeutic challenge. *Eye* 2006. 20: 1196–1206.
- 3 Yan, J., Wu, Z. and Li, Y., The differentiation of idiopathic inflammatory pseudotumor from lymphoid tumors of orbit: analysis of 319 cases. *Orbit* 2004. 23:245–254.
- 4 Yuen, S. J. A. and Rubin, P. A. D., Idiopathic orbital inflammation. *Arch. Ophthalmol.* 2003. 121: 491.
- 5 Ben Simon, G. J., Cheung, N., McKelvie, P., Fox, R. and McNab, A. A., Oral chlorambucil for extranodal, marginal zone, B-cell lymphoma of mucosa-associated lymphoid tissue of the orbit. *Ophthalmology*. 2006. 113: 1209–1213.
- 6 Eenhorst, C. A. E., Laban, K. G., Leguit, R. J., Radstake, T. R. D. J. and Kalmann, R., Orbital lymphomas missed by first biopsies of orbital masses. *Acta Ophthalmol.* 2017. 95: 858–859.
- 7 Lam Choi, V. B., Yuen, H. K. L., Biswas, J. and Yanoff, M., Update in pathological diagnosis of orbital infections and inflammations. *Middle East Afr. J. Ophthalmol.* 2011. 18: 268–276.
- 8 Mombaerts, I., Bilyk, J. R., Rose, G. E., McNab, A. A., Fay, A., Dolman, P. J., Allen, R. C. et al., Consensus on diagnostic criteria of idiopathic orbital inflammation using a modified Delphi approach. *JAMA Ophthalmol.* 2017. 135: 769–776.
- 9 Mombaerts, I., Goldschmeding, R., Schlingemann, R. O. and Koornneef, L., What is orbital pseudotumor? *Surv. Ophthalmol.* 41: 66–78.
- 10 Sachen, K. L., Strohmaier, M. J., Singletary, J., Alizadeh, A. A., Kattah, N. H., Lossos, C., Mellins, E. D. et al., Self-antigen recognition by follicular lymphoma B-cell receptors. *Blood*. 2012. 120: 4182–4190.
- 11 Burger, J. A., Ghia, P., Rosenwald, A. and Caligaris-Cappio, F., The microenvironment in mature B-cell malignancies: a target for new treatment strategies. *Blood*. 2009. 114: 3367–3375.
- 12 Gonzalez, D., van der Burg, M., Garcia-Sanz, R., Fenton, J. A., Langerak, A. W., Gonzalez, M., van Dongen, J. J. M. et al., Immunoglobulin gene rearrangements and the pathogenesis of multiple myeloma. *Blood*. 2007. 110: 3112–3121.
- 13 Kempf, W., Kerl, H. and Kutzner, H., CD123-positive plasmacytoid dendritic cells in primary cutaneous marginal zone B-cell lymphoma: a crucial role and a new lymphoma paradigm. *Am. J. Dermatopathol.* 2010. 32: 194–196.
- 14 Olsen, T. G., Holm, F., Mikkelsen, L. H., Rasmussen, P. K., Coupland, S. E., Esmaili, B., Finger, P. T. et al., Orbital lymphoma—an international multicenter retrospective study. *Am. J. Ophthalmol.* 2019. 199: 44–57.
- 15 Kase, S., Ishijima, K., Uraki, T., Suimon, Y., Suzuki, Y., Kase, M. and Ishida, S., Usefulness of flow cytometry in diagnosis of IgG4-related ophthalmic disease and extranodal marginal zone B-cell lymphoma of the ocular adnexa. *Anticancer Res.* 2017. 37: 5001–5004.
- 16 Monaco, G., Lee, B., Xu, W., Mustafah, S., Hwang, Y. Y., Carré, C., Burdin, N. et al., RNA-Seq signatures normalized by mRNA abundance allow absolute deconvolution of human immune cell types. *Cell Rep.* 2019. 26: 1627–1640.e7.
- 17 Newman, A. M., Liu, C. L., Green, M. R., Gentles, A. J., Feng, W., Xu, Y., Hoang, C. D. et al., Robust enumeration of cell subsets from tissue expression profiles. *Nat. Methods* 2015. 12: 453–457.
- 18 Musumeci, A., Lutz, K., Winheim, E. and Krug, A. B., What Makes a pDC: Recent Advances in Understanding Plasmacytoid DC Development and Heterogeneity. *Front. Immunol.* 2019. 10. <https://doi.org/10.3389/fimmu.2019.01222>.
- 19 Galati, D., Corazzelli, G., De Filippi, R. and Pinto, A., Dendritic cells in hematological malignancies. *Crit. Rev. Oncol. Hematol.* 2016. 108: 86–96.
- 20 Hillen, M. R., Ververs, F. A., Kruize, A. A. and Van Roon, J. A., Dendritic cells, T-cells and epithelial cells: a crucial interplay in immunopathology of primary Sjögren's syndrome. *Expert Rev. Clin. Immunol.* 2014. 10: 521–531.
- 21 Affandi, A. J., Carvalheiro, T., Radstake, T. R. D. J. and Marut, W., Dendritic cells in systemic sclerosis: Advances from human and mice studies. *Immunol. Lett.* 2018. 195: 18–29.
- 22 Klarquist, J., Zhou, Z., Shen, N. and Janssen, E. M., Dendritic cells in systemic lupus erythematosus: from pathogenic players to therapeutic tools. *Mediat. Inflamm.* 2016. 2016: 1–12.
- 23 Verhagen, F. H., Hiddingh, S., Rijken, R., Pandit, A., Leijten, E., Olde Nordkamp, M., ten Dam-van Loon, N. H. et al., High-dimensional profiling reveals heterogeneity of the Th17 subset and its association with systemic immunomodulatory treatment in non-infectious uveitis. *Front. Immunol.* 2018. 9: 2519.
- 24 Mohty, M., Isnardon, D., Vey, N., Brière, F., Blaise, D., Olive, D. and Gagner, B., Low blood dendritic cells in chronic myeloid leukaemia patients correlates with loss of CD34<sup>+</sup>/CD38<sup>-</sup> primitive haematopoietic progenitors. *Br. J. Haematol.* 2002. 119: 115–118.
- 25 Dong, R., Gwynarski, K., Entwistle, A., Marelli-Berg, F., Dazzi, F., Simpson, E., Goldman, J. M. et al., Dendritic cells from CML patients have altered actin organization, reduced antigen processing, and impaired migration. *Blood* 2003. 101: 3560–3567.
- 26 Orsini, E., Guarini, A., Chiaretti, S., Mauro, F. R. and Foa, R., The circulating dendritic cell compartment in patients with chronic lymphocytic leukemia is severely defective and unable to stimulate an effective T-cell response. *Cancer Res.* 2003. 63: 4497–506.
- 27 Saulep-Easton, D., Vincent, F. B., Le Page, M., Wei, A., Ting, S. B., Croce, C. M., Tam, C. et al., Cytokine-driven loss of plasmacytoid dendritic cell function in chronic lymphocytic leukemia. *Leukemia*. 2014. 28: 2005–2015.
- 28 Brimnes, M. K., Svane, I. M. and Johnsen, H. E., Impaired functionality and phenotypic profile of dendritic cells from patients with multiple myeloma. *Clin. Exp. Immunol.* 2006. 144: 76–84.
- 29 Galati, D., Zanotta, S., Corazzelli, G., Bruzzese, D., Capobianco, G., Morelli, E., Arcamone, M. et al., Circulating dendritic cells deficiencies as a new biomarker in classical Hodgkin lymphoma. *Br. J. Haematol.* 2019. 184: 594–604.
- 30 Saxena, M. and Bhardwaj, N., Re-emergence of dendritic cell vaccines for cancer treatment. *Trends Cancer* 2018. 4: 119–137.
- 31 Lombardi, V., Speak, A. O., Kerzerho, J., Szely, N. and Akbari, O., CD8 $\alpha$ <sup>+</sup> $\beta$ <sup>-</sup> and CD8 $\alpha$ <sup>+</sup> $\beta$ <sup>+</sup> plasmacytoid dendritic cells induce Foxp3<sup>+</sup> regulatory T cells and prevent the induction of airway hyper-reactivity. *Mucosal Immunol.* 2012. 5: 432–443.
- 32 Shaw, J., Wang, Y.-H., Ito, T., Arima, K. and Liu, Y.-J., Plasmacytoid dendritic cells regulate B-cell growth and differentiation via CD70. *Blood* 2010. 115: 3051–3057.
- 33 Rosenbaum, J. T., Choi, D., Wilson, D. J., Grossniklaus, H. E., Sibley, C. H., Harrington, C. A., Planck, S. R. et al., Molecular diagnosis of orbital inflammatory disease. *Exp. Mol. Pathol.* 2015. 98: 225–229.
- 34 Choi, S.-C., Kim, K. D., Kim, J.-T., Kim, J.-W., Yoon, D.-Y., Choe, Y.-K., Chang, Y.-S. et al., Expression and regulation of NDRG2 (N-myc downstream regulated gene 2) during the differentiation of dendritic cells. *FEBS Lett.* 2003. 553: 413–418.
- 35 Schraml, B. U., van Blijswijk, J., Zelenay, S., Whitney, P. G., Filby, A., Acton, S. E., Rogers, N. C. et al., Genetic tracing via DNGR-1 expression history defines dendritic cells as a hematopoietic lineage. *Cell* 2013. 154: 843–858.

- 36 Swerdlow, S. H., Campo, E., Pileri, S. A., Harris, N. L., Stein, H., Siebert, R., Advani, R. et al., The 2016 revision of the World Health Organization classification of lymphoid neoplasms. *Blood* 2016. **127**: 2375–2390.
- 37 Mombaerts, I., Rose, G. E. and Garrity, J. A., Orbital inflammation: biopsy first. *Surv. Ophthalmol.* 2016. **61**: 664–669.
- 38 Cossarizza, A., Chang, H., Radbruch, A., Acs, A., Adam, D., Adam-Klages, S., Agace, W. W. et al., Guidelines for the use of flow cytometry and cell sorting in immunological studies (second edition). *Eur. J. Immunol.* 2019. **49**: 1457–1973.
- 39 Van Gassen, S., Callebaut, B., Van Helden, M. J., Lambrecht, B. N., Demeester, P., Dhaene, T. and Saeys, Y., FlowSOM: Using self-organizing maps for visualization and interpretation of cytometry data. *Cytometry A* 2015. **87**: 636–645.
- 40 Hahne, F., LeMeur, N., Brinkman, R. R., Ellis, B., Haaland, P., Sarkar, D., Spidlen, J. et al., flowCore: a Bioconductor package for high throughput flow cytometry. *BMC Bioinformatics.* 2009. **10**: 106.
- 41 Wilkerson, M. D. and Hayes, D. N., ConsensusClusterPlus: a class discovery tool with confidence assessments and item tracking. *Bioinformatics.* 2010. **26**: 1572–1573.
- 42 Chong, J., Soufan, O., Li, C., Caraus, I., Li, S., Bourque, G., Wishart, D. S. et al., MetaboAnalyst 4.0: towards more transparent and integrative metabolomics analysis. *Nucleic Acids Res.* 2018. **46**: W486–W494.
- 43 Rosenbaum, J. T., Choi, D., Harrington, C. A., Wilson, D. J., Grossniklaus, H. E., Sibley, C. H., Salek, S. S. et al., Gene Expression Profiling and Heterogeneity of Nonspecific Orbital Inflammation Affecting the Lacrimal Gland. *JAMA Ophthalmol.* 2017. **135**: 1156.
- 44 Barrett, T., Wilhite, S. E., Ledoux, P., Evangelista, C., Kim, I. F., Tomashevsky, M., Marshall, K. A. et al., NCBI GEO: archive for functional genomics data sets—update. *Nucleic Acids Res.* 2012. **41**: D991–D995.

**Abbreviations:** ABIS: Absolute Immune Signal · cDC: conventional DC · DLBCL: diffuse large B-cell lymphoma · EMZL: extranodal marginal zone lymphoma · FC: fold change · HC: healthy controls · IOI: idiopathic orbital inflammation · NHOL: non-Hodgkin orbital lymphoma · PBMC: peripheral blood mononuclear cells · pDC: plasmacytoid DC · SOM: self-organizing map

**Full correspondence:** Kamil G. Laban, Department of Ophthalmology, University Medical Center Utrecht, Utrecht University, Room E 03.136, P.O. Box 85500 3508 GA Utrecht, The Netherlands  
Email: K.G.laban@umcutrecht.nl

**Additional correspondence:** Jonas J. W. Kuiper, Department of Ophthalmology, University Medical Center Utrecht, Utrecht University, Room E 03.136, P.O. Box 85500 3508 GA Utrecht, The Netherlands  
Email: J.J.W.Kuiper@umcutrecht.nl

The peer review history for this article is available at <https://publons.com/publon/10.1002/eji.201948370>

Received: 26/8/2019

Revised: 21/10/2019

Accepted: 10/12/2019

Accepted article online: 16/12/2019